# Electrodynamic Vibration Suppression

S. Behrens, A. J. Fleming and S. O. R. Moheimani

School of Electrical Engineering and Computer Science
University of Newcastle NSW 2308 Australia

## ABSTRACT

This paper introduces electromagnetic shunt damping (EMSD) which is similar to piezoelectric shunt damping. EMSD has four major advantages over piezoelectric shunt damping; simple transducer manufacturing, smaller shunt voltages, long stroke and larger control forces. A novel single mode shunt control strategy is validated through experimentation on a simple electromagnetic mass spring damper system. Theoretical results are also presented.

Keywords: electromagnetic, piezoelectric, shunt, vibration, passive, damping, transducer.

## 1. INTRODUCTION

Electromagnetic transducers[1–3] can be used as actuators, sensors or both. Piezoelectric transducers[4] exhibit similar electromechanical properties to electromagnetic transducers, but have considerably different physical characteristics. Electromagnetic transducers have a much greater stroke, are physically more robust and can be manufactured to either MEMS scale,[5] or as large as a 50kN electrodynamic shaker.[6] Electromagnetic transducers have been used in the field of active vibration control of car suspension systems,[7] isolation platforms,[8] magnetic levitation[9,10] and magnetic bearings.[11]

Placing an electrical impedance across the terminals of a piezoelectric transducer, which is bonded to a mechanical structure with the view to minimizing structural vibrations, is referred to as piezoelectric shunt damping.[12–16] This has been proven to be a reliable alternative to active piezoelectric vibration control techniques,[4,17] offering the benefits of stability and performance without the need of additional sensors. Most importantly, the inherent robustness makes shunt control techniques very desirable. Another desirable characteristic is collocation,[18] which also enhances the closed loop stability.

This paper presents a new shunt method for reducing structural vibration; electromagnetic shunt damping (EMSD). By attaching an electromagnetic transducer to a mechanical structure and shunting the transducer with an electrical impedance, similar to piezoelectric shunt damping,[12–16] mechanical energy can be dissipated. As the mechanical structure deforms due to some type of external disturbance, an opposing electro-motive-force (emf) is induced in the shunted transducer. Using an appropriately designed electrical shunt the electromagnetic transducer is capable of significantly reducing mechanical vibration. Compared to piezoelectric shunt damping, EMSD offers larger stroke, physical robustness, smaller shunt voltages, and can generate larger control forces.

The paper is organized as follows. Section 2 introduces a method for modeling an electromagnetic transducer and a forced mass spring damper system. In Section 3, the composite structural dynamics are derived from first principles, i.e. EMSD is modeled for a simple electromagnetic mass spring damper, while in Section 4, the composite system is derived in transfer function form for an autonomous system. Section 5 develops a single mode electromagnetic shunt impedance controller. Simulated and experimental results verify the presented work in Section 6. The paper is then concluded in Section 7.

Corresponding author: S. Behrens: E-mail: sbehrens@ecemail.newcastle.edu.au; Telephone: +61 2 4921 7223. Fax: +61 2 4921 7058

# 2. BACKGROUND

## 2.1. Electromagnetic Transducer Model

When an electrical conductor, in the form of a coil, moves in a magnetic …eld as shown in Figure 1 (a), a voltage $V_e$ proportional to the velocity $\dot{x}_e$ is induced and appears across the terminals of the coil, i.e. $V_e \_ \dot{x}_e$. Speci…cally,

$$\frac{V_e}{\dot{x}_e} = Bl; \tag{1}$$

where B is the magnetic ‡ux (in Teslas), l is the length of the conductor (in meters), and $\dot{x}_e$ is the velocity of the conductor relative to the magnetic …eld (in m/s). A permanent magnet is usually the source of the magnetic …eld.

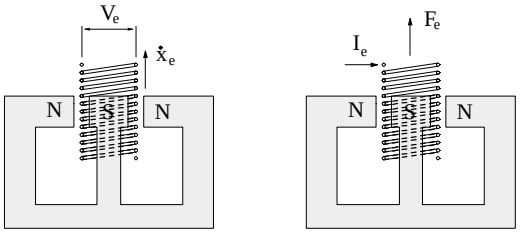


(a) (b)

Figure 1: Electromagnetic transducer, (a) sensor and (b) actuator.

Equation (1) can ideally be rewritten as,[2]

$$\frac{V_e}{\dot{x}_e} = \frac{F_e}{I_e} = Bl = C_n \tag{2}$$

where $F_e$ denotes the force (in Newtons) acting on the coil whilst carrying a current $I_e$ (in Amps), and $C_n$ is the ideal electro-mechanical coupling coe¢cient. As shown in Figure 1 (b), when the coil is employed as a force actuator, Equation (2) relates the induced force to an applied current. Such designs form the basis for electrodynamic shakers and acoustic actuators, such as a speaker coil.

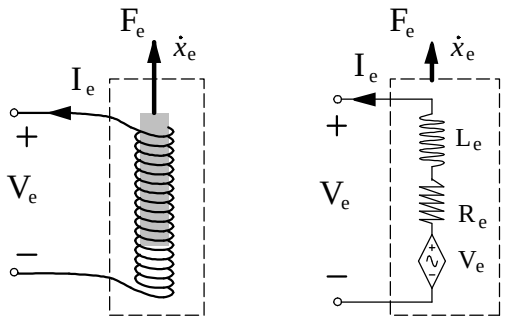


(a) (b)

Figure 2: Electromagnetic transducer (a) mechanical model and (b) electrical model.

Equation (2) can be simpli…ed with the assumption that the electromagnetic transducer operates in its linear region, i.e. undergoes only small displacements. As shown in Figure 2 (a), the coil can be modeled as series

connection of an inductor $L_e$, a resistor $R_e$ and a dependent voltage source $V_e$.[3] If the transducer is attached to a resonant mechanical system, the voltage source $V_e$, represents the induced emf that is dependent on relative velocity $\underline{\dot{x}}_e$, and hence structural dynamics.

## 2.2. Forced Mass Spring Damper System

In many cases where vibration becomes an issue, the mechanical structure can be modeled as a simple mass spring damper system, as shown in Figure 3 (a). The equivalent mass M (in Kg), spring constant K (in N/m) and damping constant C (in Ns/m) for such a structure can be easily determined. The equation of motion for this forced one degree of freedom system is given by:

$$M\ddot{x}(t) + C\underline{\dot{x}}(t) + Kx(t) = F_d(t); \tag{3}$$

where $\ddot{x}(t)$, $\underline{\dot{x}}(t)$ and $x(t)$ are the acceleration, velocity and displacement of the mass respectively. Note that $F_d(t)$ is the applied force disturbance. The dimensionless representation of equation (3) is

$$\ddot{x}(t) + 2\zeta_n \omega_n \underline{\dot{x}}(t) + \omega_n^2 x(t) = f_d(t); \tag{4}$$

where $\omega_n$ is the natural frequency of the system, and $\zeta_n$ is the damping ratio. Note that $\omega_n = \sqrt{\frac{K}{M}}$, $\zeta_n = \frac{C}{4MK}$ and $f_d(t) = \frac{F_d(t)}{M}$.

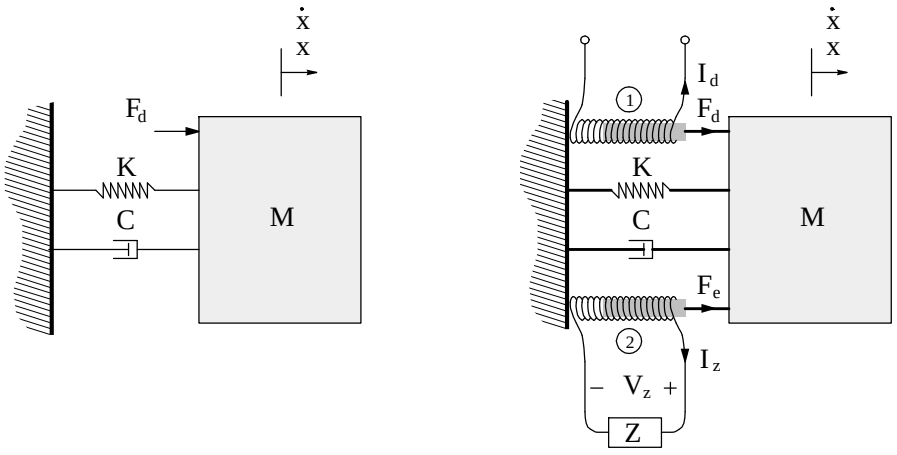


Figure 3: (a) Mass spring damper system and (b) electromagnetic shunted mass spring damper system.

# 3. STRUCTURAL DYNAMICS FROM FIRST PRINCIPLES

## 3.1. Model System

Consider Figure 3 (b), where an electromagnetic transducer (coil 1) is attached to a mass. If a current $I_d(t)$ is applied to a linear electromagnetic transducer, a disturbance force $F_d(t)$ is induced such that, $F_d(t) = C_d I_d(t)$, where $C_d$ is the electromagnetic coupling coefficient relating the applied current to a resulting force in coil 1. Using the equation of motion, the disturbed system has the following relationship, $M\ddot{x}(t) + C\underline{\dot{x}}(t) + Kx(t) = C_d I_d(t)$.

By taking the Laplace transform, the transfer functions relating the current $I_d(s)$ to displacement $x(s)$, and the current $I_d(s)$ to velocity $sx(s)$ are,

$$G_{xi}(s) \quad , \quad \frac{x(s)}{I_d(s)} = \frac{C_d}{Ms^2 + Cs + K}; \tag{5}$$

$$G_{\underline{\dot{x}}i}(s) \quad , \quad \frac{sx(s)}{I_d(s)} = \frac{C_d s}{Ms^2 + Cs + K}: \tag{6}$$

These equations are valid when coil 2, is held in open circuit, i.e. $Z(s) = 1$, as shown in Figure 3 (b).

## 3.2. Composite System

For an electromagnetic shunted composite system, as shown in Figure 3 (b), an impedance Z is attached to coil 2. we have the following relationship, $M\ddot{x}(t) + C\dot{x}(t) + Kx(t) = F_d(t) - F_e(t)$, where $F_e(t)$ is the opposing force due to the impedance Z attached to the terminals of the electromagnetic transducer. In the Laplace domain, we have the following relationship,

$$x(s)(Ms^2 + Cs + K) = C_d I_d(s) - F_e(s); \tag{7}$$

where $I_d(s)$ is the input current applied to coil 1, as shown in Section 3.1.

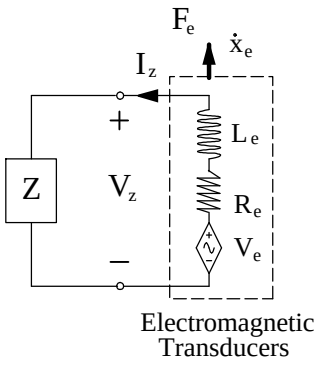


Figure 4: Simpli…ed model of the electromagnetic shunt.

To determine the opposing force $F_e(s)$, we need to consider the simpli…ed electrical model of the electromagnetic shunt, as shown in Figure 4. Ohm's law states that

$$V_z(s) = I_z(s)Z(s); \tag{8}$$

where $V_z(s)$ is the voltage across the terminals of the shunt impedance $Z(s)$, and $I_z(s)$ is the corresponding current. According to Kirchho¤'s voltage law, we obtain the following relationship between $V_e(s)$ and $V_z(s)$, as $V_z(s) = V_e(s) - (L_e s + R_e)I_z(s)$ which implies

$$V_z(s) = \frac{Z(s)}{Z(s) + L_e s + R_e} V_e(s): \tag{9}$$

As shown in equation (1), we have the following linear relationship

$$V_e(s) = C_e s x(s); \tag{10}$$

where $C_e$ is the electromagnetic constant relating $sx_e(s)$ to $V_e(s)$. Since the shunted electromagnetic transducer is attached to the mass M, $sx_e(s)$ is equivalent to $sx(s)$.

By substituting, (10) into (9), we obtain

$$V_z(s) = \frac{Z(s)}{Z(s) + L_e s + R_e} C_e s x(s): \tag{11}$$

Alternatively, the current ‡owing through the shunt $I_z(s)$, is

$$I_z(s) = \frac{V_z(s)}{Z(s)} = \frac{1}{Z(s) + L_e s + R_e} C_e s x(s); \tag{12}$$

and the opposing shunt force $F_e(s) = C_e I_z(s)$, assuming a linear electromagnetic transducer, we obtain

$$F_e(s) = \frac{C_e^2}{Z(s) + L_e s + R_e} s x(s): \tag{13}$$

Substituting (13) into (7), the composite system transfer function $I_d(s)$ to $x(s)$, is

$$\hat{G}_{xi}(s) \triangleq \frac{x(s)}{I_d(s)} = \frac{C_d}{M s^2 + \left(C + \frac{C_e^2}{Z(s) + L_e s + R_e}\right) s + K}$$

$$= \frac{C_d (Z(s) + L_e s + R_e)}{(M L_e) s^3 + (M Z(s) + M R_e + C L_e) s^2 + (C Z(s) + C R_e + C_e^2 + K L_e) s + K (Z(s) + R_e)}: \tag{14}$$

or alternatively, the transfer function relating $I_d(s)$ to $sx(s)$, is

$$\hat{G}_{\dot{x}i}(s) \triangleq \frac{sx(s)}{I_d(s)} = \frac{C_d s}{M s^2 + \left(C + \frac{C_e^2}{Z(s) + L_e s + R_e}\right) s + K}$$

$$= \frac{C_d s (Z(s) + L_e s + R_e)}{(M L_e) s^3 + (M Z(s) + M R_e + C L_e) s^2 + (C Z(s) + C R_e + C_e^2 + K L_e) s + K (Z(s) + R_e)}: \tag{15}$$

## 4. COMPOSITE SYSTEM IN TRANSFER FUNCTION FORM

By modeling the system in transfer function form, we gain a greater abstraction from the underlying system. Such methods are particularly useful when dealing with higher order systems or when using models not obtained directly through physical modeling, i.e., when using models obtained by means of system identi…cation.[19] Referring to Figure 5, the models required are: $G_{\dot{x}F}(s)$, the transfer function from an applied force to the resulting velocity $\dot{x}$; and $G_{vi}(s)$, the transfer function from an applied current to the induced emf.

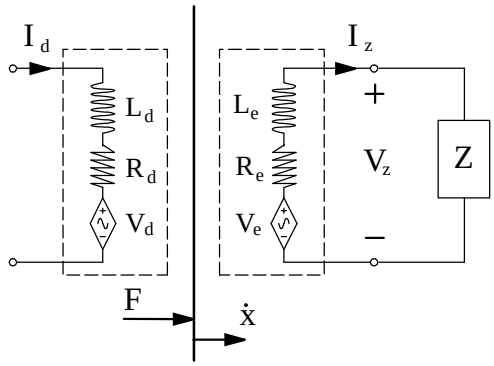


Figure 5: Electrical equivalent model of a twin coil electromagnetic system.

Considering …rst the case where two identical coils experience the same velocity. When an impedance $Z(s)$ is attached to coil 2, $V_z(s) = V_e(s) - (L_e s + R_e) I_z(s)$,

$$V_z(s) = \frac{Z(s)}{Z(s) + L_e s + R_e} V_e(s); \tag{16}$$

$$I_z(s) = \frac{1}{L_e s + R_e + Z(s)} V_e(s): \tag{17}$$

By considering the emf induced in both coils 1 and 2, and applying the principle of superposition,

$$V_e(s) = G_{vi}(s)I_d(s) - G_{vi}(s)I_z(s): \tag{18}$$

Substituting (17) yields,

$$V_e(s) = G_{vi}(s)I_d(s) - G_{vi}(s)\frac{V_e(s)}{L_e s + R_e + Z(s)}: \tag{19}$$

Hence, the composite transfer function relating $I_d(s)$ to $V_e(s)$ is

$$G_{vi}(s) \triangleq \frac{V_e(s)}{I_d(s)} = \frac{G_{vi}(s)}{1 + K(s)G_{vi}(s)}; \tag{20}$$

where

$$K(s) = \frac{1}{L_e s + R_e + Z(s)}: \tag{21}$$

The reader will appreciate that the damped system transfer function $G_{vi}(s)$ is in the form of a feedback system where the impedance $Z(s)$ parameterizes a controller $K(s)$, as shown in Figure 6 (a).

The open loop transfer function $G_{vi}(s)$ consists of both the structural dynamics and the electromagnetic coupling,

$$G_{vi}(s) = C_e G_{\dot{x}i}(s) = C_e^2 G_{\dot{x}F}(s): \tag{22}$$

In a more general case, we wish to know the damped transfer function $G_{\dot{x}F}(s)$ from some disturbance force $F(s)$ to the resulting velocity $sx(s)$. This is easily found,

$$G_{\dot{x}i}(s) \triangleq \frac{sx(s)}{I_d(s)} = \frac{V_e(s)}{I_d(s)}\frac{sx(s)}{V_e(s)} = G_{vi}(s)\frac{sx(s)}{V_e(s)} = \frac{G_{\dot{x}i}(s)}{1 + K(s)G_{vi}(s)}: \tag{23}$$

Thus,

$$G_{\dot{x}F}(s) \triangleq \frac{sx(s)}{F(s)} = \frac{sx(s)}{C_e I_d(s)} = \frac{1}{C_e}G_{\dot{x}i}(s); \tag{24}$$

and,

$$sx(s) = \frac{G_{\dot{x}i}(s)}{1 + K(s)G_{vi}(s)}I_d(s) + \frac{G_{\dot{x}F}(s)}{1 + K(s)G_{vi}(s)}F(s); \tag{25}$$

as shown in Figure 6 (b). If coils are not identical, where $G_{vi}(s)$ is transfer function from the current in coil 2 to the induced emf, and $G_{\dot{x}i}(s)$ is the transfer function from the current in coil 1 to the velocity.

## 5. SINGLE MODE ELECTROMAGNETIC SHUNT CONTROLLER

When a piezoelectric transducer is shunted by a passive electrical network, it acts as a medium for dissipating mechanical energy of the attached structure. Hagood and von Flotow[13] suggested that a series resistor-inductor circuit attached across the conducting surfaces of a piezoelectric transducer can be tuned to dissipate mechanical energy of a host structure. They demonstrated the effectiveness of this technique by tuning the resulting resistor-inductor and inherit capacitance of the piezoelectric transducer, to a specific resonance frequency of the host structure.

For electromagnetic shunt damping, we can apply the same methodology as suggested above. For this particular system, though, we need to apply resistor-capacitor circuit to the terminal of the electromagnetic transducer. That is, $Z(s) = \frac{1}{C_{ap}s} + R$, where $C_{ap} = \frac{1}{\omega_n^2 L_e}$. Therefore, the shunted electromagnetic transducer $sx(s)$ is related to $F_e$ via

$$F_e(s) = \frac{\frac{C_e^2}{L_e}s}{s^2 + \frac{R_t}{L_e}s + \frac{1}{C_{ap}L_e}}sx(s): \tag{26}$$

It should be noted that the controller has a resonant structure, as shown in (26), where $R_t = (R_e + R)$ determines the controller damping and $\omega_n$ is the resonance frequency of the mechanical structure to be damped.

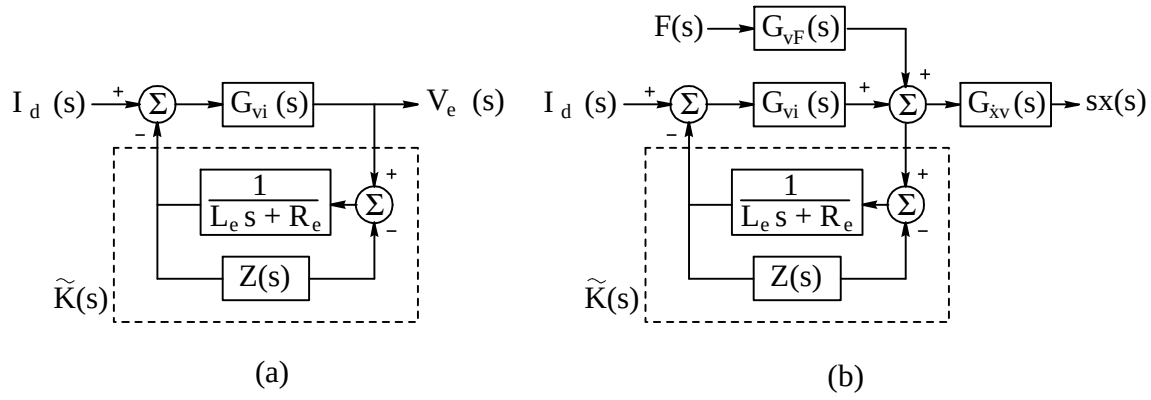


Figure 6: Electromagnetic shunt damping feedback structure: (a) Equation (20) and (b) Equation (25).

The closed loop composite transfer function between current-to-velocity $\hat{G}_{\dot{x}i}(s)$, is

$$\hat{G}_{\dot{x}i}(s) \triangleq \frac{sx(s)}{I_d(s)} = \frac{C_d s}{Ms^2 + \left(C + \dfrac{\frac{C_e^2}{L_e}s}{s^2 + \frac{R_t}{L_e}s + \frac{1}{C_{ap}L_e}}\right)s + K} \tag{27}$$

or alternatively,

$$G_{\dot{x}i}(s) \triangleq \frac{sx(s)}{I_d(s)} = \frac{G_{\dot{x}i}(s)}{1 + \tilde{K}(s)G_{vi}(s)} \tag{28}$$

where $\tilde{K}(s) = \dfrac{\frac{1}{L_e}s}{s^2 + \frac{R_t}{L_e}s + \frac{1}{C_{ap}L_e}}$.

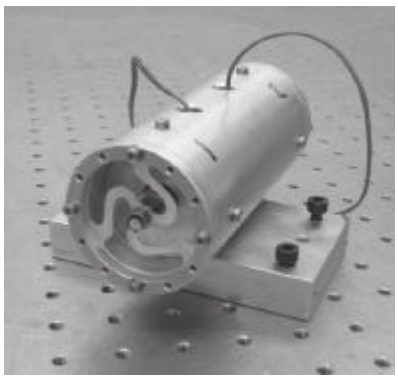

Figure 7: An external photograph of the experimental electromagnetic apparatus.

## 6. EXPERIMENTAL VERIFICATION OF ELECTROMAGNETIC SHUNT DAMPING CONCEPT

### 6.1. Electromagnetic Transducer Design

In support of the preceding sections, the technique of electromagnetic shunt damping was applied to an experimental assembly at the Laboratory for Dynamics and Control of Smart Structures in The University of

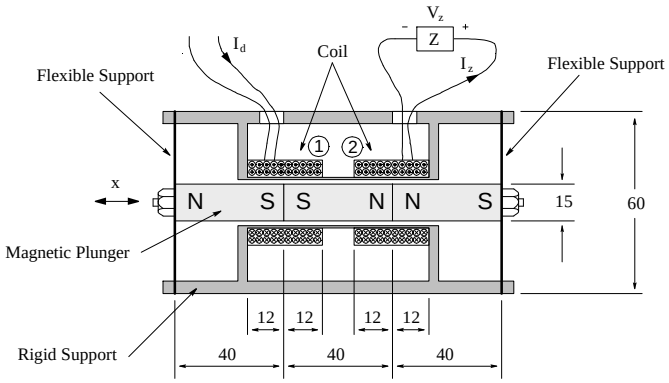


Figure 8: Side section of the experimental electromagnetic apparatus. (All dimensions in mm)

Newcastle, Australia [¤]. A photograph of the electromagnetic transducer apparatus, showing the rigid external support, flexible end supports, mounting plate, coils and winding cables is provided in Figure 7. As shown in Figure 8, the assembly is essentially a translational solenoid with two identical fixed coils and a magnetic plunger supported at either end by flexible supports. This system is mechanically equivalent to the mass spring damper shown in Figure 3. Together with an attached electrical impedance $Z(s) = \frac{1}{C_{ap}s} + R$, coil 2 is employed to damp translational vibrations resulting from an applied disturbance current $I_d$ to coil 1.

In practice, the magnetic field strength, as well as being a function of the magnetic material, is limited by the maximum allowable dimensions and weight of the magnets. In these experiments, three rare earth magnets (Neodymium Iron Boron), are arranged to form the magnetic plunger, as shown in Figure 8. At the two points where opposing poles meet (at the center of each winding), a strong magnetic field exits at right angles to the plunger. When the plunger is in motion, the strong parallel field flowing through the coil results in a high flux density and corresponding large induced force.

Each coil is wound from 0:25 mm diameter enamel coated copper wire and has an electrical impedance of 3:3 - and 1 mH. Non-magnetic materials, such as aluminum and copper, were used in the construction of the rigid external support, flexible end supports and the mounting plate. Non-magnetic materials were utilized so as to prevent the magnetic disturbance.

| Parameter | Value |
|---|---|
| Spring constant K | 56 kN m$^{-1}$ |
| Damping coefficient C | 2:667 N sm$^{-1}$ |
| Plunger mass M | 0:150 kg |
| Electromagnetic Coupling $C_d$ | 3:65 |
| Electromagnetic Coupling $C_e$ | 3:4 |
| Coil Inductance $L_e$ | 1 mH |
| Coil Resistance $R_e$ | 3:3 - |

Table 1: Electromechanical system parameters.

## 6.2. Determining Optimal Damping Resistance

The electromechanical model $G_{\bar{x}i}(s)$ was first determined by measuring the resonance frequency and plunger weight M, and subsequently determine the spring constant K. The remaining parameter $!_n$, together with the electromagnetic coupling coefficients $C_d$ and $C_e$, were determined experimentally. A summary of the model parameters is provided in Table 1. The frequency response from an applied current to the resulting plunger

[¤] http://rumi.newcastle.edu.au/lab

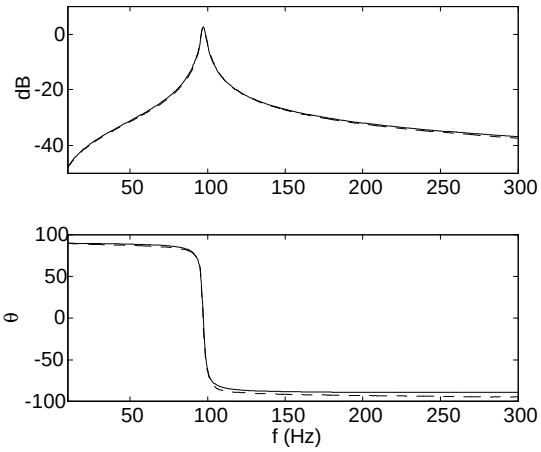


Figure 9. The open loop frequency response from an applied actuator current to plunger velocity, i.e. $G_{\dot{x}i}(s)$, model (–) and measured results (- -).

velocity $G_{\dot{x}i}(s)$; is shown in Figure 9. It is observed that the model is an accurate representation of the physical system.

Since we wish to damp the fundamental frequency of the mass spring damper system, i.e. $!_n = 97{:}3\ Hz$, the required shunt capacitance value is $C_{ap} = 2{:}6\ mF$.

In order to determine an appropriate value for the total shunt resistance $R_t$, an optimization approach was used to minimize the $H_2$ norm of the closed loop system $G_{\dot{x}i}(s)$. This required a solution to the following optimization problem to be found;

$$R_t^{¤} = \arg \min_{R_t > 0} \left\| G_{\dot{x}i}(s) \right\|_2 : \tag{29}$$

Using the proposed optimization strategy the required optimal shunt resistance $R_t^{¤} = 0{:}29\ \Omega$, and alternatively $R_t^{¤}$ can be found by plotting $H_2$ norm against $R_t$, as shown in Figure 10.

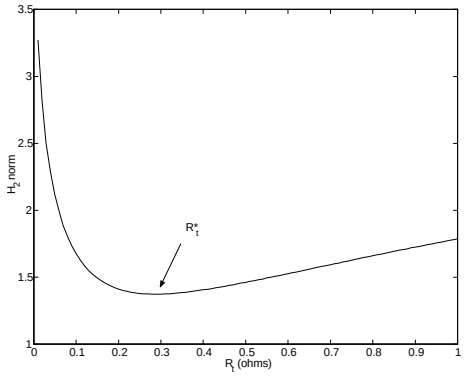


Figure 10: $\left\| G_{\dot{x}i}(s) \right\|_2$ against $R_t$ (-).

## 6.3. Impedance Implementation

To implement the proposed arbitrary shunt impedance $Z(s)$, a current controlled voltage source was utilized, as shown in Figure 11. The controlled voltage $v_z$ was set to be a function of the measured current $i_z$, i.e., $v_z(t) = f(i_z(t))$, as shown in Figure 11 (a). If the function $f(i_z(t))$, is a linear transfer function $Z(s)$ whose

input impedance is the measured current $I_z(s)$, i.e., $V_z(s) = Z(s)I_z(s)$, then the terminal impedance $Z_t(s)$ is equal to $Z(s)$, as shown in Figure 11 (b). For a more detailed description of the impedance apparatus, the reader is referred to Fleming et. al..[20, 21]

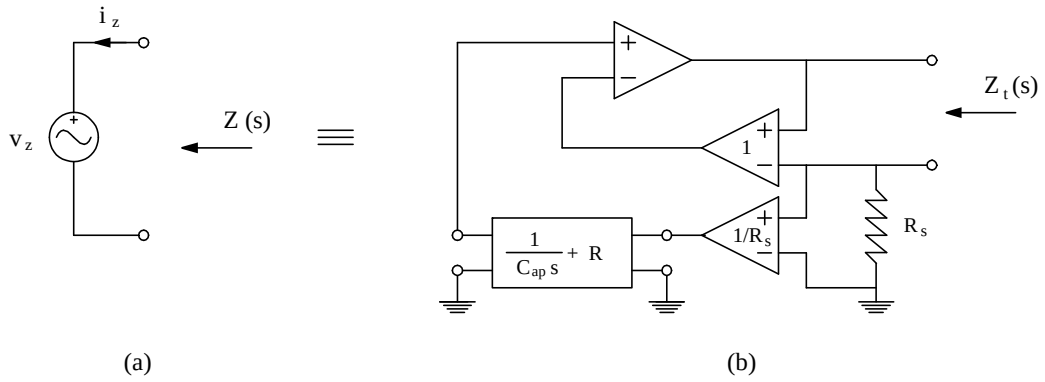


Figure 11: (a) Ideal current controlled voltage source, and (b) experimental current controlled voltage source.

## 6.4. Simulated vs Experimental Results

With the aim of damping the system, a total series resistance ($R_e + R$) of 0:35 - and a capacitance 27 mF were applied to the second winding using the synthetic impedance appartus explained in Section 6.3. The measured open loop, theoretically predicted damped, and measured damped frequency responses are shown in Figure 12. A signi…cant reduction of 21:8 dB in the magnitude of the electromechanical system is observed. The e¤ect of such reduction greatly decreases the settling time of the system. Figure 13 shows the undamped response of the system to a 1 A low pass …ltered step in actuator current. In comparison, the damped response shown in Figure 14 settles in less than one tenth of the time taken by the undamped system.

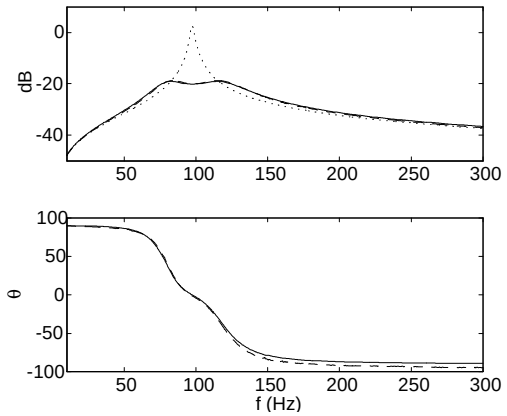


Figure 12. The open loop (¢¢¢), theoretically predicted damped (–), and measured damped (- -) frequency responses from an applied current to the resulting plunger velocity.

A summary of simulated and experimental parameters are tabulated in Table 2. Simulated and experimental results closely agree, therefore validating the proposed electromagnetic shunt damping.

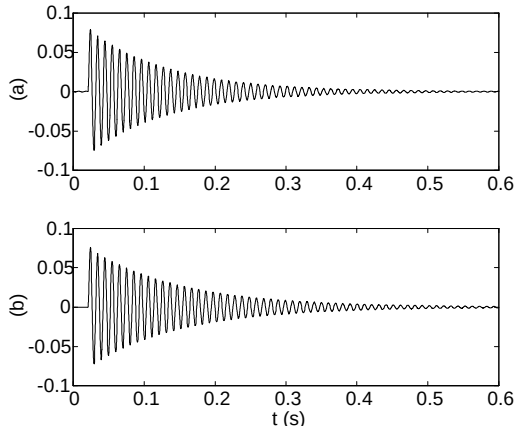


Figure 13. Velocity response of the system to a 1 A low pass …ltered step in actuator current. (a) theoretically predicted, and (b) experimental.

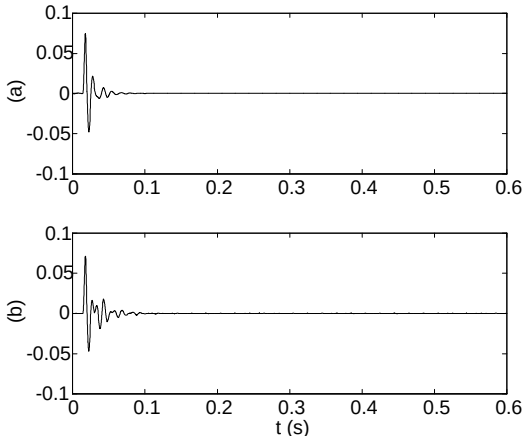


Figure 14. Damped response of the system to a 1 A low pass …ltered step in actuator current. (a) theoretically predicted, and (b) experimental.

## 7. CONCLUSIONS

In this paper we have introduced a new type of vibration control, electromagnetic shunt damping (EMSD). The proposed technique is similar to piezoelectric shunt damping, as a shunt impedance is attached to the terminals of an electromagnetic transducer. Electromagnetic shunt damping has many advantages, compared to piezoelectric shunt damping; it is physically robust, has a greater stroke and can damp much larger structures. The proposed technique was experimentally validated on a simple electromagnetic mass spring damper system.

| Parameter | Simulated | Experimental |
|---|---|---|
| Total Resistance $R_t$ (-) | 0:29 | 0:35 |
| Capacitance $C_{ap}$ (mF) | 2:6 | 2:7 |
| Amplitude reduction (dB) | 21:8 | 21:8 |
| Time Decaly | 1=10 | 1=10 |

Table 2: Shunt impedance parameters.

A 21:8 dB peak amplitude reduction was achieved via simulation and experimentation.

## 8. ACKNOWLEDGMENTS

This research was supported by the Centre for Integrated Dynamics and Control (CIDAC) and the Australian Research Council (ARC).

## REFERENCES

1. S. Mirzaei, S. M. Saghaiannejad, V. Tahani, and M. Moallem, "Linear electric actuators and generators," IEEE Transaction on Energy Conversion 14, pp. 712 –717, September 1999.
2. S. S. Rao, Mechanical Vibrations, Addison-Wesley Publishing Company, 3rd ed., 1995.
3. B. M. Hanson, M. D. Brown, and J. Fisher, "Self sensing: Closed-loop estimation for a linear electromagnetic actuator," in Proc. IEEE American Control Conference, pp. 1650–1655, (Arlington, VA USA), June 2001.
4. C. R. Fuller, S. J. Elliott, and P. A. Nelson, Active Control of Vibration, Academic Press, 1996.
5. R. Amirtharajah and A. P. Chandrakasan, "Self-powered signal processing using vibration-based power generation," IEEE Journal of Solid-State Circuits 33, pp. 687–695, May 1998.
6. Gearing and Watson Electronics Ltd., South Road, Hailsham, E Sussex BN27 3JJ England, Large Shaker Model No. V53-64/DSA4. http://www.gearing-watson.com.
7. Y. B. Kim, W. G. Hwang, C. D. Kee, and H. B. Yi, "Active vibration control of suspension system using an electromagnetic damper," in Proc. of the I MECH E part D Journal of Automoblie Engineering (Professional Engineering Publishing), 215(8), pp. 865–873, 2001.
8. J. Shaw, "Active vibration isolation by adaptive control," in Proc. IEEE International Conference on Control Applications, pp. 1509–1514, (Hawaii, USA), August 1999.
9. D. Vischer and H. Bleuler, "Self-sensing active magnetic levitation," IEEE Transactions on Magnetics 29(2), pp. 169–177, 1993.
10. C. Choi and K. Park, "Self-sensing magnetic levitation using LC resonant circuits," Sensors and Actuators , pp. 1276–1281, 1999.
11. N. Morse, R. Smith, and B. P. J. Antaki, "Position sensed and self-sensing magnetic bearing con…guations and associated robustness limitations," in Proc. IEEE Conference on Decision and Control, pp. 2599–2604, (Tampa, Florida USA), December 1998.
12. R. L. Forward, "Electronic damping of vibrations in optical structures," Applied Optics 18, pp. 690–697, March 1979.
13. N. W. Hagood and A. Von Flotow, "Damping of structural vibrations with piezoelectric materials and passive electrical networks," Journal of Sound and Vibration 146(2), pp. 243–268, 1991.
14. D. L. Edberg, A. S. Bicos, C. M. Fuller, J. J. Tracy, and J. S. Fechter, "Theoretical and experimental studies of a truss incorporating active members," Journal of Intelligent Materials Systems and Structures 3, pp. 333–347, 1992.
15. S. Behrens and S. O. R. Moheimani, "Current ‡owing multiple mode piezoelectric shunt dampener," in Proc. SPIE Smart Materials and Structures, Paper No. 4697-24, pp. 217–226, (San Diego, CA), March 2002.
16. S. Behrens, S. O. R. Moheimani, and A. J. Fleming, "Multiple mode current ‡owing passive piezoelectric shunt controller," Accepted for Publication in: Journal of Sound and Vibration , 2002.
17. G. S. Agnes, "Active/passive piezoelectric vibration suppression," in Proc. SPIE Smart Structures and Materials, Passive Damping, SPIE Vol. 2193, pp. 24–34, (San Diego, CA), May 1994.
18. D. G. MacMartin, "Collocated structural control: motivation and methodology," in Proc. IEEE International Conference on Control Applications, pp. 1092–1097, (Albany, New York USA), September 1995.
19. L. Ljung, System Identi…cation: Theory for the User, Prentice Hall, 1999.
20. A. J. Fleming, S. Behrens, and S. O. R. Moheimani, "Synthetic impedance for implementation of piezoelectric shunt-damping circuits," Electronics Letters 36, pp. 1525–1526, August 2000.
21. A. Fleming and S. O. R. Moheimani, "Improved current and charge ampli…ers for driving piezoelectric loads, and issues in signal processing design for synthesis of shunt damping circuits.," Journal of Intelligent Material Systems and Structures , Submitted August 2002.